Investigation of Flow Separation on a Supercritical Airfoil

B. H. K. Lee*
National Research Council, Ottawa, Ontario, Canada

Transonic shock/boundary-layer interaction on the upper surface of a supercritical airfoil was investigated in the National Aeronautical Establishment High Reynolds Number Two-Dimensional Test Facility. Skin-friction coefficient measurements on the airfoil surface were carried out using a Preston tube. At the lower Mach number range of the experiments, shock-induced and trailing-edge separation regions were found to exist simultaneously. Detailed experimental measurements were carried out at $M = 0.688$ and various values of α to investigate the merging of the two separated-flow regions. Steady and unsteady pressure measurements were made for various types of shock/boundary-layer interaction. Pressure power spectra were computed to study the characteristics of pressure fluctuations in the separated-flow regions. Fluctuating normal forces were measured for different types of flow separation, and the behavior of the unsteady load experienced by the airfoil was presented. Broadband cross-correlations of the pressure field were carried out to determine the convection velocities for attached and separated flows.

Nomenclature

b	= model span
C_f	= skin-friction coefficient
C_L	= lift coefficient
C_N	= fluctuating normal-force coefficient from balance measurement
C'_N	= rms value of normal-force coefficient
C_p	= pressure coefficient, p/q_∞
C_{p_s}	= steady-state pressure coefficient
C'_p	= rms value of pressure coefficient
c	= chord
M	= Mach number
N_{rms}	= rms value of normal force from balance measurement
p	= instantaneous pressure
p_{rms}	= rms value of unsteady pressure
q_∞	= freestream dynamic pressure
$R(a,b,\tau)$	= cross-correlation of functions a and b
U_c	= broadband convection velocity
U_∞	= freestream velocity
x	= distance measured in flow direction from airfoil leading edge
α	= angle of incidence
τ	= time delay

Introduction

THE types of flow separation on conventional airfoils were systematically classified by Pearcey et al.[1] from analysis of steady pressure measurements on the airfoil surface. Recently, Mundell and Mabey[2] presented some steady and unsteady pressure data on shock-induced separation of turbulent boundary layers on a 12%-thick NACA 16 series airfoil. Their results supplemented the classification of the types of flow separation described by Pearcey.[1]

The unsteady data obtained by Mundell and Mabey[2] covered a small region on the airfoil surface. Only six fast-response transducers were installed on the upper airfoil surface between 45 and 70% chord, and their spacings were not sufficiently close to resolve the rapid changes in the separated-flow regions. Their results are useful in buffet studies since they provide a guide to the types of unsteady excitation on the airfoil arising from the pressure fluctuations. However, more detailed experiments are required to give quantitative results, which are needed to understand the dynamics of flow separation so that accurate estimation of loads on the airfoil can be made. This is required in order to predict the structural response of the airfoil in the investigation of buffeting flows.

Some recent experiments of flow separation on a supercritical airfoil were performed at the National Aeronautical Establishment (NAE) High Reynolds Number Two-Dimensional Test Facility. The Bauer-Garabedian-Korn (BGK) No. 1 supercritical airfoil, which was used in previous buffet studies,[3] was modified by the installation of 16 fast-response transducers from 20 to 87% chord on the airfoil upper surface. Pressure fluctuations due to shock-induced and trailing-edge separation were measured. From these data, intensities and power spectra were computed. Broadband correlations of the pressure field were also carried out to determine the convection velocities. Skin-friction measurements using a Preston tube were performed to determine the separated-flow regions. The dimensions of these separated-flow regions were compared with those obtained from steady pressure data or from curves

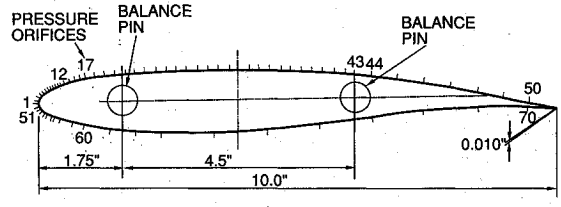

Fig. 1a Schematic of BGK No. 1 supercritical airfoil with pressure orifice locations.

TRANSDUCER	E	F	G	H	I	J	K	L
x (in.)	2.00	2.50	3.00	3.50	4.00	4.50	5.00	5.50
TRANSDUCER	M	N	O	P	Q	R	S	T
x (in.)	5.91	6.32	6.73	7.14	7.55	7.96	8.37	8.7

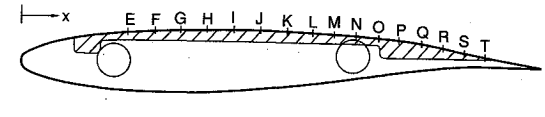

Fig. 1b Locations of fast-response transducers on the upper surface of the BGK No. 1 supercritical airfoil.

Received Feb. 28, 1989; revision received May 12, 1989. Copyright © 1989 by B. H. K. Lee. Published by the American Institute of Aeronautics and Astronautics, Inc., with permission.

*Senior Research Officer, National Aeronautical Establishment, High Speed Aerodynamics Laboratory. Member AIAA.

of pressure fluctuation intensities with distance on the airfoil surface. The unsteady pressure results gave further support to the types of flow separation that can be classified in the manner suggested by Mundell and Mabey.[2]

Model, Instrumentation, and Data Reduction

The airfoil tested was the BGK No. 1 with design M and C_L of 0.75 and 0.63, respectively. The chord of the airfoil was 10 in. and the span was 15 in. The thickness-to-chord ratio was 11.8%. Figure 1a shows a schematic of the airfoil. There were 50 pressure orifices on the airfoil upper surface and 20 on the lower surface for steady pressure measurements. A modification of the original airfoil was made, and this involved milling off a 0.75-in.-wide, 8-in.-long groove from the upper surface 2.5 in. from the centerline. A replacement insert was made, and 16 25-psid miniature Kulite differential transducers with a 0.062-in. diam were installed. The locations of these transducers are given in Fig. 1b. The second transducer located 2.5 in. from the airfoil leading edge was found to be defective. It was not used in the tests.

The rms value of the fluctuating pressure p_{rms} is normalized by q_∞ and is given as

$$C_p' = p_{\text{rms}}/q_\infty \tag{1}$$

The lift and pitching moment were determined by use of a sidewall balance. In addition to the steady-state values of the balance outputs, the fluctuating quantities were also measured. The rms value on the normal force is presented in coefficient form given by the expression

$$C_N' = N_{\text{rms}}/q_\infty bc \tag{2}$$

Spectral analyses of the transducers and balance outputs were performed. The signals were sampled at 1.6 kHz and analyzed digitally on a computer using the Institute of Electrical and Electronics Engineers (IEEE) routine periodgram method for power spectrum estimation (PMPSE).[4] Two modes of operation were used for the tunnel runs, namely, step-pause incidence runs and constant incidence runs. For the first mode of operation, a fast Fourier transform (FFT) size of 256 and a signal duration of 2 s were chosen in determining the power spectra. For the second mode, the transform size was 1024 and approximately 10 s of the signal were processed. For cross-correlation studies, the pressure transducer signals were recorded on a FM tape recorder at 60 in./s and analyzed at a reduced speed of 3.75 in./s. The IEEE program correlation method for power spectrum estimation (CMPSE)[4] was used to compute the correlation functions.

In Ref. 5, it was reported that distinct peaks of about 70–80 Hz for Mach numbers between 0.688 and 0.747 were observed from the force and pressure power spectra for this airfoil. These were attributed to shock wave oscillations in a region beyond the buffet onset boundary where the flow was fully separated. The force balance was very stiff, and both the lowest frequencies of rigid-body airfoil heave and fixed-fixed wing bending were much larger than the observed peak excitation frequencies at about 70–80 Hz. No wind-off test was performed for this airfoil, but tests performed for another supercritical airfoil[6] using the same balance showed the first four balance natural frequencies to be approximately 140, 215, 320, and 360 Hz, respectively. These were all greater than the 70–80 Hz observed in this test. Also, dynamic calibration of the transducers with impulse excitation did not show any frequency peaks.

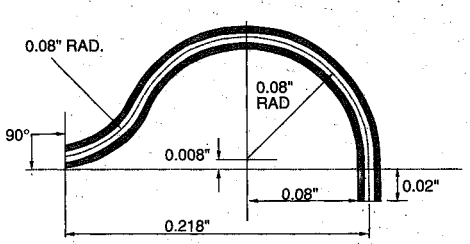

Fig. 2 Schematic of Preston tube.

A fast-response pressure transducer was installed on the sidewall of the wind tunnel to measure the unsteady tunnel pressure. It was located approximately 26 in. upstream of the airfoil leading edge. From the measured power spectra,[7] a discrete frequency of approximately 420 Hz was detected. The magnitude of this pressure oscillation depended on M and α of the airfoil. The origin of this flow disturbance so far has not been identified from the NAE tunnel.

For skin-friction measurements, a Preston tube with dimensions given in Fig. 2 was used. It was constructed from a hypodermic needle having a 0.0165 in. o.d. and a 0.004 in. wall thickness. The probe could be installed at any desired pressure orifice location. The pitot pressure on the airfoil surface was measured. The corresponding local surface static pressure was obtained by interpolation of the static pressures obtained on the airfoil surface ahead and behind the Preston tube. From the difference between the total and static pressures, the calibration chart given by Head and Ram[8] was used to determine the skin-friction coefficient. To obtain the C_f distribution on the airfoil surface, only one Preston tube was used at a fixed location for each wind-tunnel run to minimize any disturbance from the probe. The probe location was then changed and the run was repeated with the same flow conditions. Because of the large number of wind-tunnel runs required to find the surface distribution of C_f, measurements were carried out for $M = 0.688$ only. The location closest to the leading edge where measurements were taken was $0.3c$. The step-pause mode of wind-tunnel testing was used, and ten values of α were considered. The range of α covered attached to fully separated flows.

Distributed suction was applied through porous plates to regions of the tunnel sidewalls in the vicinity of the model. The amount of suction was selected so as to minimize any three-dimensional effects.[9] All tests were performed at a chord Reynolds number of approximately 20×10^6 with free transition. At design conditions, previous tests showed transition on the airfoil upper surface to occur within 10% chord from the leading edge. The Mach numbers in this investigation ranged from 0.5 to 0.792.

Results and Discussions

Skin-Friction Coefficient Measurements

For the BGK No. 1 supercritical airfoil, it is found that at the lower Mach number range of the experiments, separation can begin as a bubble behind the shock wave and spread downstream as the angle of incidence is increased. Trailing-edge separation occurs when α reaches a certain value. The rear separation region moves upstream and will merge with the shock-induced separated-flow region.

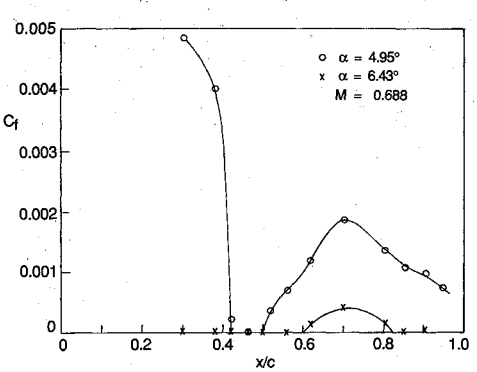

Fig. 3 Skin-friction coefficient vs x/c at $M = 0.688$ and $\alpha = 4.95$ and 6.43 deg.

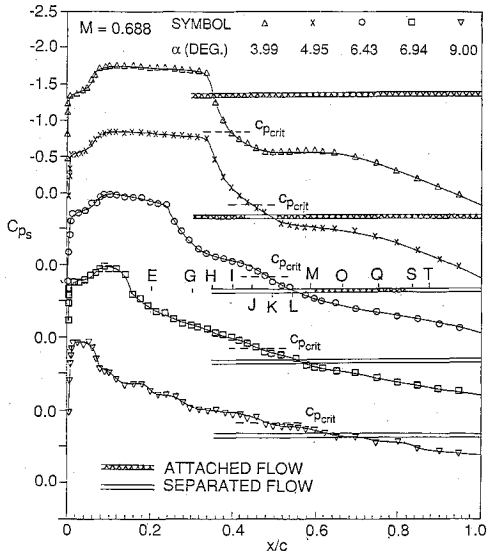

Fig. 4 Steady-state pressure distributions on upper surface of BGK No. 1 airfoil at various α. The cross-hatched and open bar symbols denote regions of attached and separated flows determined from Preston tube measurements.

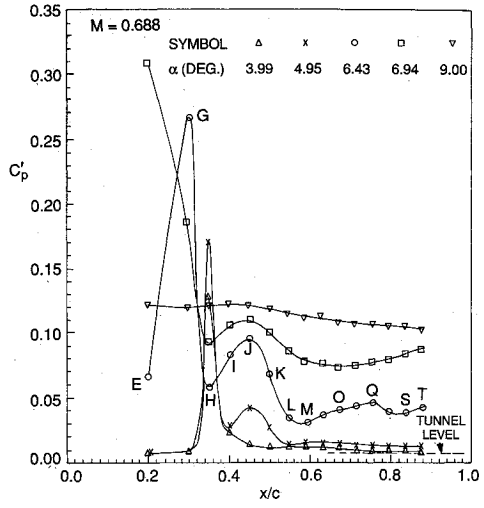

Fig. 5 Variations of pressure intensities on upper surface of BGK No. 1 airfoil at various α.

The sequence of events observed experimentally for the range of α values selected in this test at $M = 0.688$ can be summarized as follows. At $\alpha = 4.67$ deg, a small separation bubble behind the shock wave is observed. Increasing α to 4.95 deg, the flow is attached from the leading edge to x/c—approximately 0.42. Figure 3 shows the dimension of the shock-induced separation bubble, given by $C_f = 0$, as approximately 0.08c. The spacing of the Preston tube was not sufficiently close to give very accurate measurements of the dimension of the separation bubble. The spatial resolution for the skin-friction measurements was at best 0.05c for x/c greater than 0.6 and 0.02c for values of x/c between 0.3 and 0.6. This was dictated by the location of the pressure orifices on the airfoil surface.

When the angle of incidence is increased to 5.92 deg, the separation bubble has moved only slightly from its position at $\alpha = 4.95$ deg, and the flow is still attached at the trailing edge. At the next test value of α, which is 6.13 deg, trailing-edge separation has already occurred and the separation point is at $x/c = 0.89$. The trailing-edge separation region moves rapidly toward the leading edge as α is increased. At $\alpha = 6.43$ deg, the average shock position is located at approximately 0.26c (Fig. 4). No skin-friction measurements were taken for x/c at less than 0.3. Hence, values of C_f for the attached flow upstream of the shock wave are not available for this value of α. The C_f distribution in Fig. 3 shows the two separated-flow regions to be approximately 0.23c apart. It is interesting to note that the trailing-edge separated-flow region moves upstream much faster than the downstream motion of the shock-induced separation bubble. The difference in α when the flow changes from rear separation at $x/c = 0.89$ to fully separated at the shock is approximately 0.8 deg. The next selected value of α in the test is 6.67 deg. The results show the two separated-flow regions to be very close, and the distance between them is about 0.08c. At $\alpha = 6.94$ deg, the two regions have completely merged and the flow is fully separated.

Classification of the Types of Shock/Boundary-Layer Interaction

Mundell and Mabey[2] classified shock/boundary-layer interaction to be of three types. The first involves a weak shock that interacts with the turbulent boundary layer, resulting in a low-level excitation close to the shock. A short distance downstream of the shock, the pressure fluctuations revert to the empty tunnel level.

Results for the BGK No. 1 airfoil corresponding to the described type of interaction is shown in Fig. 4 in the form of C_{p_s} distribution on the upper surface of the airfoil at $M = 0.688$ and $\alpha = 3.99$ deg. The curves for different α are displaced downward by one unit of the vertical scale to avoid overlapping. Skin-friction measurements between 30 and 95% chord showed the flow to be attached. The pressure fluctuations are shown in Fig. 5, where the peak intensity occurs behind the shock wave at $x/c = 0.35$. The pressure intensity decreases very rapidly behind the shock to a value close to the tunnel level. There was a small variation in the tunnel pressure intensities with airfoil incidence, and the value shown in Fig. 5 is the average for α between 3.99 and 9 deg.

Increasing the incidence to 4.95 deg results in the formation of a small bubble at the shock/boundary interaction region. The C_f distribution given in Fig. 3 shows a small bubble at x/c from approximately 0.42 to 0.5. At this value of α, Fig. 5 shows that in addition to the large peak behind the shock wave, there is a second peak of smaller magnitude located at x/c of about 0.45. The second peak is slightly in front of the center of the separated-flow bubble determined from Preston tube measurements. This type of flow corresponds to the second class of shock/boundary-layer interactions described by Mundell and Mabey.[2] The stronger shock wave at $\alpha = 4.95$ deg causes the flow to separate locally at the shock/boundary-layer interaction region. The flow then reattaches to form a bubble. The pressure fluctuation levels are practically constant in the reattached region, which extends to the trailing-edge of the airfoil. They are slightly higher than the tunnel level averaged for the values of α considered. Experimental results are only given up to $x/c = 0.87$, which was the location of the transducer closest to the trailing edge.

The C_{p_s} distribution on the airfoil upper surface given in Fig. 4 at $\alpha = 6.43$ deg shows a shock-induced separation bubble between $x/c = 0.36$ and 0.6. Preston tube measurements indicated trailing-edge separation to occur at the position $x/c = 0.82$. The location of the rear separated-flow region is not readily detectable from steady pressure measurements. The corresponding pressure intensity plot is given in Fig. 5. The separation bubble is given by the curve "HIJKLM." The peak pressure intensity inside the bubble occurs at transducer J, which is slightly in front of the center of the separated-flow region. The intensity reaches a minimum at transducer M, which is very close to the reattachment point determined from skin-friction measurements (Fig. 4). Because of the spatial inaccuracies in the Preston tube measurements, the reattached-flow region probably extends further upstream to include the position where transducer M was located.

Increasing α to 6.94 deg causes the flow to be fully separated. It is seen that the intensity distribution behind the shock

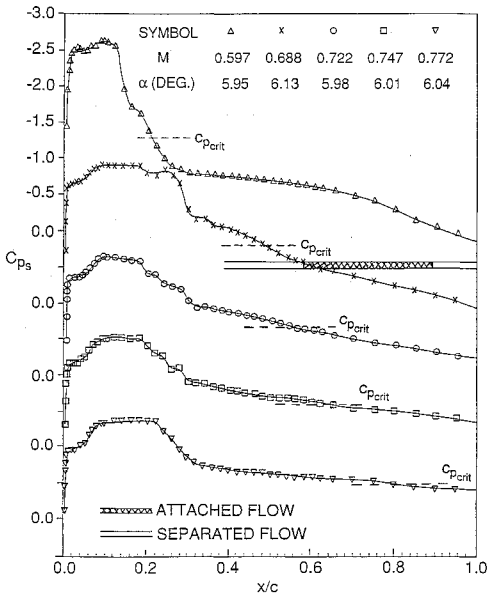

Fig. 6 Steady-state pressure distributions on upper surface of BGK No. 1 airfoil at various M. The cross-hatched and open bar symbols denote regions of attached and separated flows determined from Preston tube measurements.

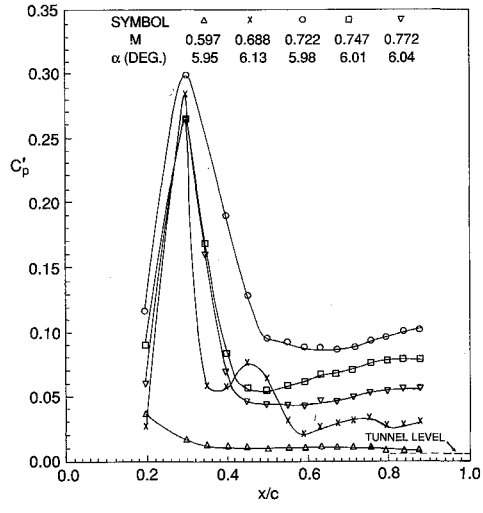

Fig. 7 Variations of pressure intensities on upper surface of BGK No. 1 airfoil at various M.

wave (Fig. 5) still shows a bulge typical for flows with a separation bubble. Skin-friction measurements show that the two separated-flow regions have just merged and the flow is fully separated. At this stage of flow separation, some of the characteristics of the separation bubble and rear separation region are still preserved. The flow corresponds to the third type of shock/boundary interactions described by Mundell and Mabey.[2] At $\alpha = 9$ deg, the flow becomes very unsteady, and large shock wave motion is detected. A typical intensity distribution curve for large-scale separation is shown in Fig. 5. A very gradual decrease in the pressure fluctuation intensity toward the trailing edge is seen.

The effect of Mach number on the type of shock/boundary-layer interaction is illustrated in Figs. 6 and 7. M varies from 0.597 to 0.772 and α is about 6 deg. No skin-friction measurements were performed for M other than 0.688. The types of separation can be deduced from C_{p_s} plots. At $M = 0.597$ and $\alpha = 5.95$ deg, the flow is attached. Increasing the Mach number to 0.688, skin-friction measurements at $\alpha = 6.13$ deg show a separation bubble occurring at a position approximately

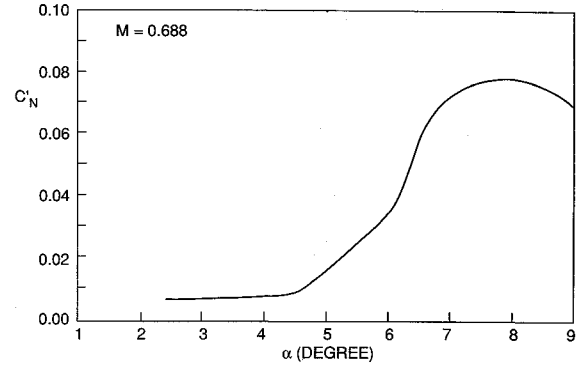

Fig. 8 Variations of C'_N with α at $M = 0.688$.

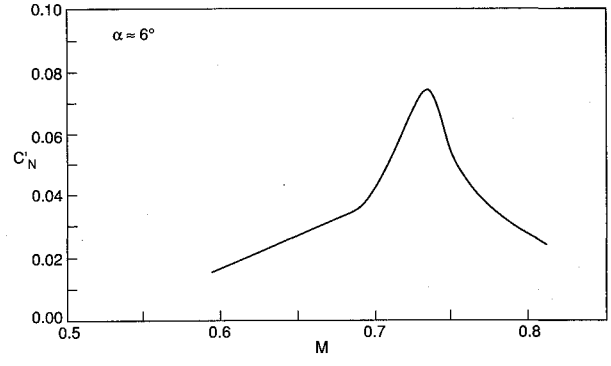

Fig. 9 Variations of C'_N with M at α, approximately 6 deg.

between 0.38 and 0.58c downstream of the airfoil leading edge. Trailing-edge separation is detected at x/c of about 0.89. At the higher Mach numbers, the pressure fluctuation intensity curves do not show the characteristic bulge associated with a separation bubble, as shown for $M = 0.688$. The flow is fully separated from the shock to the trailing edge of the airfoil.

Fluctuating Normal Force Measurements

The rms values of the normal force coefficient measured from the balance are shown in Fig. 8 for $M = 0.688$. The changes in C'_N with α are very small when the flow is attached. From the skin-friction results, a shock-induced bubble is first detected at α of approximately 4.67 deg. The bubble grows with increasing α. At $\alpha = 6.13$ deg, trailing-edge separation has reached the position $x/c = 0.89$, and at $\alpha = 6.94$ deg, the flow is fully separated downstream of the shock wave. The exact α when trailing-edge separation begins is not known. It is seen from Fig. 8 that the slope of the curve changes at $\alpha \simeq 6$ deg. Since the increase in C'_N through the range of α from 4.67 to 6 deg is primarily due to the fluctuating pressures acting on the airfoil inside the separation bubble, it can be assumed that trailing-edge separation occurs at α of about 6 deg. For α between 6 and 6.94 deg, the fluctuating force is due to the unsteady pressures inside the separation bubble and trailing-edge separation region. The later moves rapidly upstream with increasing α, and hence, the slope of the C'_N vs α curve is greater than that below $\alpha = 6$ deg. Above 6.94 deg, C'_N increases slowly to a maximum and then decreases with further increase in α. The results given in Ref. 5 show that at $M = 0.688$, discrete frequency shock oscillations cease to exist when the maximum value of α reaches approximately 8 deg. Figure 8 shows C'_N reaches its maximum at this α. For α greater than 8 deg, there is no contribution to C'_N from the pressure field associated with discrete shock wave oscillations.

The behavior of C'_N with Mach number at $\alpha =$ approximately 6 deg is shown in Fig. 9. A maximum occurs at $M =$ approximately 0.733. Previous studies[3] of the buffet

characteristics of this airfoil show that large fluctuating normal force occurs at about this Mach number. From Ref. 5, it is shown that between $M = 0.615$ and 0.67, no discrete shock oscillations are present. From $M = 0.67$–0.69, only weak shocks exist. The slope of the C_N' vs M curve for $0.615 < M < 0.69$ is smaller than that for $0.69 < M < 0.733$, where fairly strong shock oscillations occur in the latter range of M. At the higher values of Mach numbers ($M > 0.733$), the shock weakens and the pressure field due to shock oscillations decreases with increasing M, resulting in a decrease in C_N'.

Power Spectra of Unsteady Pressure Fluctuations

Figure 10 shows the variations of pressure spectra in the various regions of interest at $M = 0.688$ and $\alpha = 6.43$ deg. The transducer locations on the airfoil surface where the spectra are computed are marked on Figs. 4 and 5 for reference purposes. The peak at 70 Hz is seen at all transducer locations downstream of the shock wave.

The pressure power spectra are presented in three sets. The first (Fig. 10a) gives the spectra in front of and behind the shock wave. Except in the vicinity of the large peak at 70 Hz, which is due to shock wave oscillation, the spectra at transducer G are approximately 7 dB higher than at transducer E. The spectra inside the separation bubble are given by transducers H–M, and are shown in Fig. 10b. Each curve is displaced 10 dB downward so that they do not overlap. The spectra at transducers I and J are very similar except for frequencies below 50 Hz, where a slightly higher level is detected for J. The values of the 70-Hz peak for these three curves are very close, but at frequencies below 200 Hz, there is a slight increase in the spectral level for I and J above that of H. From transducers K–M, the magnitude of the 70-Hz peak and the level of the spectra below 200 Hz decrease with increasing distance from J.

In the reattachment region, representative spectra are given in Fig. 10c by transducers O and Q. The two curves are very similar, and comparison with Fig. 10b shows that they are very close to the pressure spectra for M. In the trailing-edge separation region, the spectra for transducers S and T show little difference from those in the reattached-flow region.

Broadband Correlation of Pressure Field

Two-point broadband cross-correlations of the pressure field were performed to determine the convection velocities of the pressure field. The pressure transducer signals were analyzed on a digital computer using the IEEE routine CMPSE.[4] From the correlation functions, the convection velocity can be computed knowing the separation distance between transducers and the time delay τ for the peaks of the cross-correlation functions to pass over them.

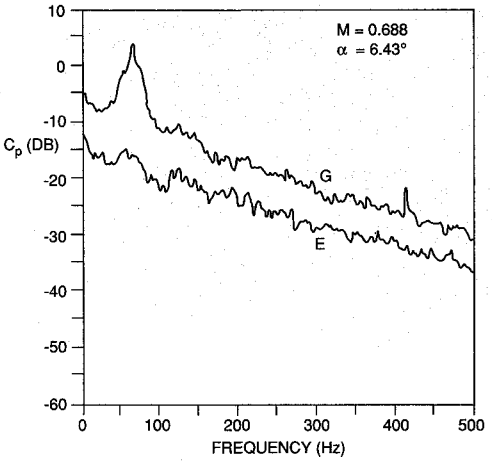

Fig. 10a Power spectra of unsteady pressure on upper surface of BGK No. 1 airfoil for transducers located before and after shock.

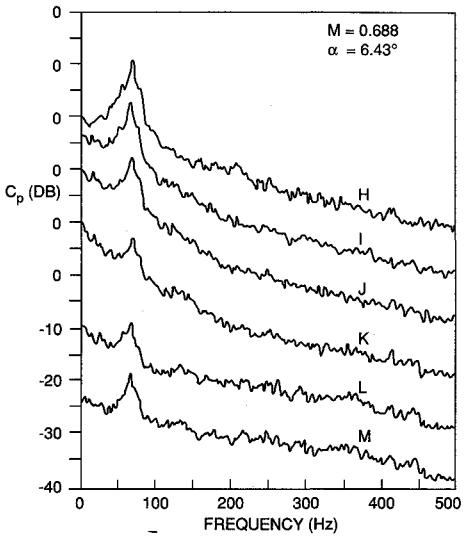

Fig. 10b Power spectra of unsteady pressure on upper surface of BGK No. 1 airfoil for transducers located in the separation bubble.

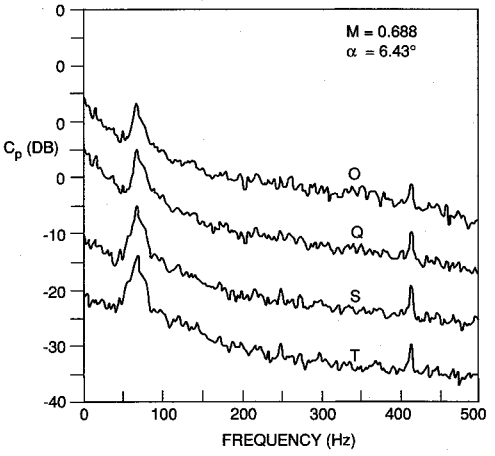

Fig. 10c Power spectra of unsteady pressure on upper surface of BGK No. 1 airfoil for transducers located in the reattached and trailing-edge separation regions.

Figure 11a shows the cross-correlation functions at $M = 0.688$ and $\alpha = 3.99$ deg. The last transducer T located at $x/c = 0.87$ was used as the reference. The flow is attached and the figure shows an upstream propagation of pressure disturbance similar to the observations made by Roos.[10] The average velocity for this case is $U_c/U_\infty = 0.255$. Increasing α to 6.43 deg, both shock-induced and trailing-edge separations occur simultaneously. The cross-correlation functions shown in Fig. 11b are coherent only in a region close to the last transducer location. The convection velocity is in the downstream direction, and the average value of U_c/U_∞ is 0.858.

At $\alpha = 9$ deg, the flow is fully separated. Figure 11c shows that the pressure field is coherent for quite a large distance from $x/c = 0.87$. The calculated value of U_c/U_∞ is 0.532. It is seen that the convection velocity decreases with increasing α, or when flow separation becomes more and more severe. Figure 12 shows the variations of U_c/U_∞ with α for different Mach numbers. For large values of α, all the curves reach a constant value of U_c/U_∞ between 0.5 and 0.55. No narrowband cross-correlation were carried out, and hence, comparisons with related studies[10] are not possible.

Conclusions

Three types of shock/boundary-layer interactions are described in this investigation. Trailing-edge separation can oc-

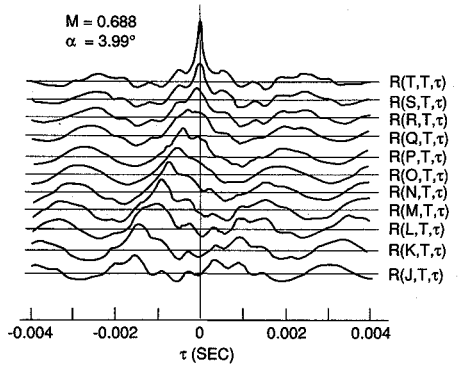

Fig. 11a Cross-correlation functions of pressure field at $M = 0.688$ and $\alpha = 3.99$ deg.

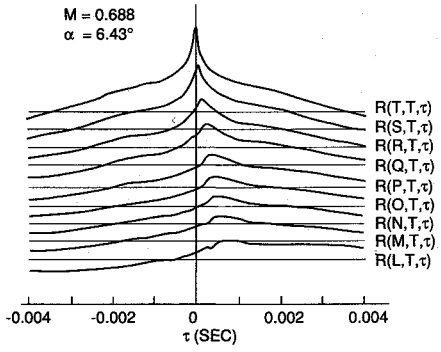

Fig. 11b Cross-correlation functions of pressure field at $M = 0.688$ and $\alpha = 6.43$ deg.

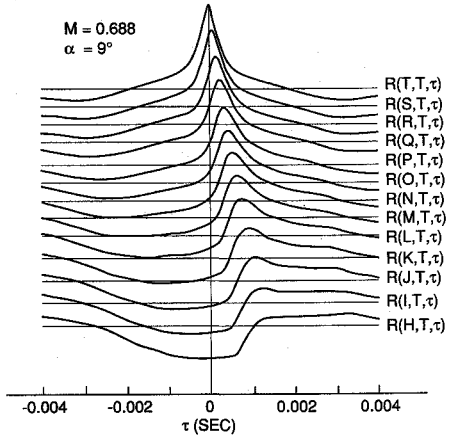

Fig. 11c Cross-correlation functions of pressure field at $M = 0.688$ and $\alpha = 9$ deg.

cur simultaneously with shock-induced separation. These two regions will merge and the flow becomes fully separated. This phenomenon is usually observed at lower Mach numbers.

The regions of separated flow can be determined from skin-friction measurements when $C_f = 0$. For shock-induced separation with reattachment, results at $M = 0.688$ show that the dimensions of the separation bubble agree very closely with those determined from the bulge in the fluctuating pressure intensity measurements on the airfoil surface. The pressure spectral level inside the separation bubble increases at frequencies below 200 Hz up to the location on the airfoil where the pressure intensity reaches a maximum. Thereafter,

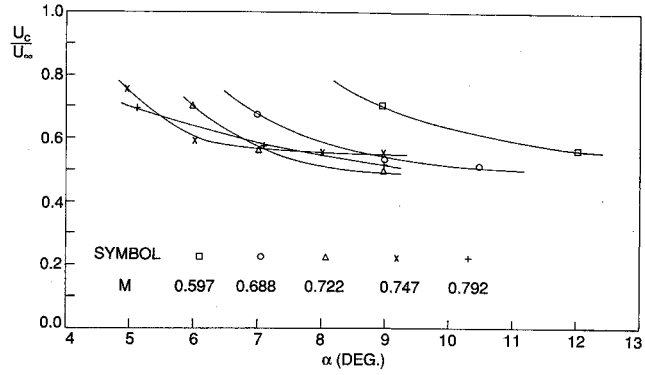

Fig. 12 Variations of normalized convection velocities with α for various M.

the level decreases toward the reattachment point. The spectra in the reattachment and trailing-edge separation regions are quite similar.

At $M = 0.688$, C_N' varies quite uniformly with α under conditions where shock-induced separation occurs. When trailing-edge separation sets in, the increase in C_N' with α is more rapid and a maximum is reached, followed by a decrease with further increase in α. The α at the maximum C_N' coincides with that when discrete shock oscillation is absent. At α, approximately 6 deg, a maximum in C_N' occurs at $M = 0.733$. Previous tests have shown that very large force fluctuations are observed at this Mach number.

Broadband cross-correlations of the pressure field show that at large α, convection velocities U_c/U_∞ between 0.5 and 0.55 are observed for $M = 0.597$–0.792.

References

[1]Pearcey, H. H., Osborne, J., and Haines, A. B., "The Interaction between Local Effects at the Shock and Rear Separation—a Source of Significant Scale Effects in Wind-Tunnel Tests on Airfoils and Wings," "Transonic Aerodynamics," Paper 11, AGARD CP 35, 1968.

[2]Mundell, A. R. G. and Mabey, D. G., "Pressure Fluctuations caused by Transonic Shock/Boundary-Layer Interaction," *Aeronautical Journal,* Vol. 90, Aug./Sept. 1986, pp. 274–281.

[3]Lee, B. H. K. and Ohman, L. A., "Unsteady Pressures and Forces During Transonic Buffeting of a Supercritical Airfoil," *Journal of Aircraft,* Vol. 21, June 1984, pp. 439–441.

[4]Rabiner, L. R., Schafer, R. W., and Dlugos, D., "Periodgram Method for Power Spectrum Estimation" and "Correlation Method for Power Spectrum Estimation," *Programs for Digital Signal Processing*, edited by the Digital Processing Committee, IEEE Acoustics, Speech and Signal Processing Society, Institute of Electrical and Electronics Engineers, New York, 1979, pp. 2.1.1–2.1.10 and 2.2.1–2.2.14.

[5]Lee, B. H. K., "Oscillatory Shock Motion Caused by Transonic Shock-Boundary Layer Interaction," *AIAA Journal,* Vol. 26, May 1989, pp. 459–464.

[6]Lee, B. H. K. and Tang, F. C., "Transonic Buffet of a Supercritical Airfoil with Trailing-Edge Flap," *Journal of Aircraft,* Vol. 26, May 1989, pp. 459–464.

[7]Lee, B. H. K., Ellis, F. A., and Bureau, J., "Investigation of the Buffet Characteristics of Two Supercritical Airfoils," *Journal of Aircraft,* Vol. 26, Aug. 1989, pp. 731–736.

[8]Head, M. R. and Ram, V. V., "Simplified Presentation of Preston Tube Calibration," *Aeronautical Quarterly,* Vol. 22, Pt. 3, Aug. 1971, pp. 295–300.

[9]Ohman, L. H., "The NAE High Reynolds Number 15″ × 60″ Two-Dimensional Test Facility," National Aeronautical Establishment LTR-HA-4, Part I, National Research Council of Canada, April 1970.

[10]Roos, F. W., "Some Features of the Unsteady Pressure Field in Transonic Airfoil Buffeting," *Journal of Aircraft,* Vol. 17, Nov. 1980, pp. 781–788.